Massive MIMO Downlink Transmission for LEO Satellite Communications

Ke-Xin Li*†, Li You*†, Jiaheng Wang*†, Xiqi Gao*†, Christos G. Tsinos§, Symeon Chatzinotas§, and Björn Ottersten§

*National Mobile Communications Research Laboratory, Southeast University, Nanjing 210096, China

†Purple Moutain Laborataries, Nanjing 211100, China

§Interdisciplinary Centre for Security, Reliability and Trust (SnT), University of Luxembourg, Luxembourg City 2721, Luxembourg

Email: {likexin3488, liyou, jhwang, xqgao}@seu.edu.cn, chtsinos@gmail.com, {symeon.chatzinotas, bjorn.ottersten}@uni.lu

***Abstract*—We investigate the downlink (DL) transmit strategy for massive multiple-input multiple-output (MIMO) low-earth-orbit (LEO) satellite communication (SATCOM) systems, in which only the slow-varying statistical channel state information is known at the transmitter side. First, we establish the massive MIMO LEO satellite channel model, in which the uniform planar arrays are deployed at both the satellite and user terminals (UTs). Building on the rank-one property of satellite channel matrices, we show that transmitting a single data stream to each UT is optimal for the ergodic sum rate maximization. This result is of great importance for massive MIMO LEO SATCOM systems, since the sophisticated design of transmit covariance matrices is turned into that of precoding vectors, with no loss of optimality at all. Furthermore, we conceive an algorithm to compute the precoding vectors. Simulation results show the significant performance gains of the proposed approaches over the previous schemes.**

I. Introduction

Satellites have been recognized as one the most promising fundamental infrastructures to provide global seamless coverage [1]. Recently, low-earth-orbit (LEO) satellite communication (SATCOM) constellations have attracted intensive researchers' interests, due to their benefits on shorter delay, reduced pathloss, and lower manufacture costs [2], [3]. Nowadays, some LEO SATCOM systems have started to provide broadband high-throughput services, e.g., Starlink.

Multibeam satellites are the prevailing solutions in SATCOM systems, which serve the coverage areas with spot beams [4]. By mincing the evolution of terrestrial wireless communications, the full frequency reuse (FFR) scheme, in which all spot beams use the same frequency band [5], has been advocated in SATCOM systems to further enhance spectral efficiency. To alleviate the serious inter-beam interference, the concept of precoding techniques originated from multiuser multiple-input multiple-output (MU-MIMO) systems is introduced in multibeam SATCOM systems, e.g., [6]–[8].

The conventional beamforming network (BFN) at multibeam satellites is usually assumed to be fixed [6]–[8]. By deploying a large number of antennas at the base station (BS), massive MIMO transmission has made great success in terrestrial 5G communications, which can significantly improve the spectrum and energy efficiency [9]. Indeed, the advantages of massive MIMO hinge on the multiple reconfigurable beams. Currently, the rapid development of microwave and antenna technologies has made it possible to implement a digitally reconfigurable BFN at the satellite [10]. In this paper, we focus on an LEO satellite equipped with a large-scale antenna array, i.e., a massive MIMO LEO satellite, and we assume that the BFN at the satellite can be digitally reconfigurable.

Notice that the previous works mostly assume that the transmitter can obtain the instantaneous channel state information (iCSI) [6]–[8], [11]. Nevertheless, it is challenging to acquire the iCSI at the transmitter due to the satellite channel impairments, e.g., large propagation delays and Doppler effects. Compared with the iCSI, statistical CSI (sCSI) is stable for a longer time period [12], and thus can be more easily obtained at the transmitter side. In this paper, we assume that the satellite can only exploit sCSI for the downlink (DL) transmit design.

The DL transmit design using sCSI at the transmitter (sCSIT) has been studied in massive MIMO terrestrial cellular systems, e.g., [13]–[15]. However, these works do not consider the massive MIMO LEO satellite channel properties, and have high implementation complexity. In [16], the authors studied the channel model, DL precoders, UL receivers, and user grouping for massive MIMO LEO SATCOM systems with single-antenna user terminals (UTs). Nevertheless, the DL precoders in [16] are derived under the individual criterion of maximizing average signal-to-leakage-plus-noise ratio (ASLNR) for each UT, thus restricting the system throughput.

In this paper, we investigate the DL transmit strategy for massive MIMO LEO SATCOM system, where the satellite and the UTs are both equipped with uniform planar arrays (UPAs), by only exploiting the slow-varying sCSIT. First, we establish the DL massive MIMO LEO satellite channel model. The Doppler and delay effects are compensated at each UT to support the wideband transmission. We show that transmitting a single data stream to each UT is optimal for linear transmitters to maximize the ergodic sum rate. Then, the intricate design of transmit covariance matrices is simplified into that of precoding vectors, and an algorithm is devised to compute the precoding vectors. Simulation results verify the effectiveness of the proposed approaches.

II. System Model

A. System Setup

We consider that a massive MIMO LEO satellite at an altitude of H serves mobile UTs on ground over lower frequency bands, e.g., L/S/C bands. The satellite has a large-scale UPA with M_{x} and M_{y} elements in the x-axis and y-axis, respectively. Then, the total number of antennas at the satellite is $M_{\mathrm{x}}M_{\mathrm{y}} \triangleq M$. Each UT's UPA has $N_{\mathrm{x}'}$ and $N_{\mathrm{y}'}$ elements in the x′-axis and y′-axis, respectively, and $N \triangleq N_{\mathrm{x}'}N_{\mathrm{y}'}$ is the total number of antennas at each UT.

B. Signal and Channel Models in Analog Baseband

First, the DL received signal at UT k at time instant t can be expressed as follows

$$\mathbf{y}_k(t) = \int_{-\infty}^{\infty} \check{\mathbf{H}}_k(t,\tau)\mathbf{x}(t-\tau)\,\mathrm{d}\tau + \mathbf{z}_k(t), \quad (1)$$

where $\check{\mathbf{H}}_k(t,\tau) \in \mathbb{C}^{N\times M}$, $\mathbf{x}(t) \in \mathbb{C}^{M\times 1}$ and $\mathbf{z}_k(t) \in \mathbb{C}^{N\times 1}$ are the channel impulse response (CIR), transmit signal and additive Gaussian noise of UT k, respectively. The time-varying LEO satellite CIR $\check{\mathbf{H}}_k(t,\tau)$ can be written as

$$\check{\mathbf{H}}_k(t,\tau) = \sum_{\ell=0}^{L_k-1} a_{k,\ell} e^{j2\pi\nu_{k,\ell}t}\delta\left(\tau-\tau_{k,\ell}\right)\mathbf{d}_{k,\ell}\mathbf{g}_{k,\ell}^H, \quad (2)$$

where $j \triangleq \sqrt{-1}$, $\delta(x)$ is the Dirac delta function. In (2), L_k, $a_{k,\ell}$, $\nu_{k,\ell}$, $\tau_{k,\ell}$, $\mathbf{d}_{k,\ell} \in \mathbb{C}^{N\times 1}$ and $\mathbf{g}_{k,\ell} \in \mathbb{C}^{M\times 1}$ are the number of multipaths, complex channel gain, Doppler shift, propagation delay, array response vector at the UT side and array response vector at the satellite side, respectively, corresponding to path ℓ of UT k's channel. We assume that these channel parameters are unchanged within each coherence time interval. The detailed LEO satellite channel characteristics will be elaborated one by one as follows.

1) Doppler shifts: The Doppler shifts in LEO satellite channels are more significant than those in terrestrial wireless channels, on account of the high moving velocity of the satellite. For a LEO satellite at an altitude of 1000 km operating at the 4 GHz carrier frequency, the Doppler shift can be 80 kHz [17]. The Doppler shift $\nu_{k,\ell}$ for path ℓ of UT k's channel mainly includes two terms [18], i.e., $\nu_{k,\ell} = \nu_{k,\ell}^{\mathrm{sat}} + \nu_{k,\ell}^{\mathrm{ut}}$, where $\nu_{k,\ell}^{\mathrm{sat}}$ and $\nu_{k,\ell}^{\mathrm{ut}}$ are the Doppler shifts due to the movement of the satellite and UT k, respectively. The first term $\nu_{k,\ell}^{\mathrm{sat}}$ is almost the same for different ℓ's [18]. Hence, we have $\nu_{k,\ell}^{\mathrm{sat}} = \nu_k^{\mathrm{sat}}$, $\ell = 0,\dots,L_k-1$. Moreover, ν_k^{sat} varies almost deterministically, and hence it can be estimated and compensated at UTs. On the other hand, $\nu_{k,\ell}^{\mathrm{ut}}$'s of each path are usually different.

2) Propagation Delays: The propagation delays for LEO satellite channels are also much larger than those in terrestrial wireless channels. For a LEO satellite at an altitude of 1000 km, the round-trip delay can be about 17.7 ms [19]. The minimal and maximal propagation delays of UT k's channel is defined as $\tau_k^{\min} = \min_\ell \tau_{k,\ell}$ and $\tau_k^{\max} = \max_\ell \tau_{k,\ell}$, respectively.

3) Array response vectors: Let $\boldsymbol{\theta}_{k,\ell} = (\theta_{k,\ell}^{\mathrm{x}}, \theta_{k,\ell}^{\mathrm{y}})$ and $\boldsymbol{\varphi}_{k,\ell} = (\varphi_{k,\ell}^{\mathrm{x}'}, \varphi_{k,\ell}^{\mathrm{y}'})$ denote the paired angles-of-departure (AoDs) and paired angles-of-arrival (AoAs), respectively, for path ℓ of UT k's channel. The array response vectors $\mathbf{g}_{k,\ell}$ and $\mathbf{d}_{k,\ell}$ in (2) can be expressed as $\mathbf{g}_{k,\ell} = \mathbf{g}(\boldsymbol{\theta}_{k,\ell})$ and $\mathbf{d}_{k,\ell} = \mathbf{d}(\boldsymbol{\varphi}_{k,\ell})$, respectively, where $\mathbf{g}(\boldsymbol{\theta})$ and $\mathbf{d}(\boldsymbol{\varphi})$ for arbitrary $\boldsymbol{\theta} = (\theta_{\mathrm{x}}, \theta_{\mathrm{y}})$ and $\boldsymbol{\varphi} = (\varphi_{\mathrm{x}'}, \varphi_{\mathrm{y}'})$ are defined as $\mathbf{g}(\boldsymbol{\theta}) = \mathbf{a}_{M_{\mathrm{x}}}\left(\sin\theta_{\mathrm{y}}\cos\theta_{\mathrm{x}}\right) \otimes \mathbf{a}_{M_{\mathrm{y}}}\left(\cos\theta_{\mathrm{y}}\right)$ and $\mathbf{d}(\boldsymbol{\varphi}) = \mathbf{a}_{N_{\mathrm{x}'}}\left(\sin\varphi_{\mathrm{y}'}\cos\varphi_{\mathrm{x}'}\right) \otimes \mathbf{a}_{N_{\mathrm{y}'}}\left(\cos\varphi_{\mathrm{y}'}\right)$, respectively. In addition, $\mathbf{a}_{n_{\mathrm{v}}}(x) \in \mathbb{C}^{n_{\mathrm{v}}\times 1}$ is defined as $\mathbf{a}_{n_{\mathrm{v}}}(x) = \frac{1}{\sqrt{n_{\mathrm{v}}}}(1, e^{-j\frac{2\pi d_{\mathrm{v}}}{\lambda}x}, \dots, e^{-j\frac{2\pi d_{\mathrm{v}}}{\lambda}(n_{\mathrm{v}}-1)x})^T$, where $\lambda = c/f_c$ is the carrier wavelength, d_{v} is the spacing between adjacent antennas along v-axis with $\mathrm{v} \in \{\mathrm{x}, \mathrm{y}, \mathrm{x}', \mathrm{y}'\}$. In satellite channels, $\boldsymbol{\theta}_{k,\ell}$'s for different ℓ's are nearly the same [16], i.e., $\boldsymbol{\theta}_{k,\ell} = \boldsymbol{\theta}_k$, $\ell = 0,\dots,L_k-1$. Thus, we have $\mathbf{g}_{k,\ell} = \mathbf{g}_k = \mathbf{g}(\boldsymbol{\theta}_k)$, where $\boldsymbol{\theta}_k = (\theta_k^{\mathrm{x}}, \theta_k^{\mathrm{y}})$ is the paired physical angle of UT k. Since the distance between the satellite and UT k is far enough, $\mathbf{g}_k$ varies quite slowly. Thus, we assume that $\mathbf{g}_k$ is perfectly known at the satellite. The paired space angle $\tilde{\boldsymbol{\theta}}_k = (\tilde{\theta}_k^{\mathrm{x}}, \tilde{\theta}_k^{\mathrm{y}})$ of UT k is defined as $\tilde{\theta}_k^{\mathrm{x}} = \sin\theta_k^{\mathrm{y}}\cos\theta_k^{\mathrm{x}}$ and $\tilde{\theta}_k^{\mathrm{y}} = \cos\theta_k^{\mathrm{y}}$ [16]. The nadir angle ϑ_k of UT k is defined as $\vartheta_k = \cos^{-1}\left(\sin\theta_k^{\mathrm{y}}\sin\theta_k^{\mathrm{x}}\right) \le \vartheta_{\max}$, where $\vartheta_{\max}$ is the maximum nadir angle. The paired space angle $\tilde{\boldsymbol{\theta}}_k$ should satisfy $\sqrt{(\tilde{\theta}_k^{\mathrm{x}})^2 + (\tilde{\theta}_k^{\mathrm{y}})^2} \le \sin\vartheta_{\max}$, due to the relation $\cos\vartheta_{\max} \le \cos\vartheta_k = \sin\theta_k^{\mathrm{y}}\sin\theta_k^{\mathrm{x}} = \sqrt{1-(\tilde{\theta}_k^{\mathrm{y}})^2-(\tilde{\theta}_k^{\mathrm{x}})^2}$.

C. Signal and Channel Models for OFDM Based Transmission

The orthogonal frequency division multiplex (OFDM) technique is used to combat frequency selective fading in LEO satellite systems. The number of subcarriers and length of cyclic prefix (CP) are given by N_{sc} and N_{cp}, respectively. The system sampling period is T_{s}. Then, the time duration of CP is $T_{\mathrm{cp}} = N_{\mathrm{cp}}T_{\mathrm{s}}$. The time duration of one OFDM symbol without and with CP is given by $T_{\mathrm{sc}} = N_{\mathrm{sc}}T_{\mathrm{s}}$ and $T = T_{\mathrm{sc}} + T_{\mathrm{cp}}$, respectively.

We use $\{\mathbf{x}_{s,r}\}_{r=0}^{N_{\mathrm{sc}}-1}$ to denote the $M\times 1$ frequency-domain transmit signal in OFDM symbol s. Then, the corresponding time-domain transmit signal is given by

$$\mathbf{x}_s(t) = \sum_{r=0}^{N_{\mathrm{sc}}-1}\mathbf{x}_{s,r}e^{j2\pi r\Delta f t},\ -T_{\mathrm{cp}} \le t - sT < T_{\mathrm{sc}}, \quad (3)$$

where $\Delta f = 1/T_{\mathrm{sc}}$. Then, UT k's time-domain receiving signal in OFDM symbol s be written as

$$\mathbf{y}_{k,s}(t) = \int_{-\infty}^{\infty}\check{\mathbf{H}}_k(t,\tau)\mathbf{x}_s(t-\tau)\,\mathrm{d}\tau + \mathbf{z}_{k,s}(t), \quad (4)$$

where $\mathbf{z}_{k,s}(t)$ is the additive Gaussian noise. By performing Doppler and delay compensation at each UT [16], the compensated time-domain receiving signal of UT k in OFDM symbol s is given by

$$\mathbf{y}_{k,s}^{\mathrm{cps}}(t) = \mathbf{y}_{k,s}(t+\tau_k^{\mathrm{cps}})e^{-j2\pi\nu_k^{\mathrm{cps}}(t+\tau_k^{\mathrm{cps}})}, \quad (5)$$

where $\nu_k^{\mathrm{cps}} \triangleq \nu_k^{\mathrm{sat}}$ and $\tau_k^{\mathrm{cps}} \triangleq \tau_k^{\min}$. Hence, we can choose a suitable CP duration subject to $T_{\mathrm{cp}} \ge \tau_k^{\max} - \tau_k^{\min}$, to combat the multipath fading in LEO satellite channels. Then, UT k's frequency-domain receiving signal over subcarrier r in OFDM symbol s can be written as

$$\mathbf{y}_{k,s,r} = \frac{1}{T_{\mathrm{sc}}}\int_{sT}^{sT+T_{\mathrm{sc}}}\mathbf{y}_{k,s}^{\mathrm{cps}}(t)e^{-j2\pi r\Delta f t}\,\mathrm{d}t. \quad (6)$$

Define the channel frequency response (CFR) of UT k after the Doppler and delay compensation as

$$\mathbf{H}_k(t,f) = \mathbf{d}_k(t,f)\mathbf{g}_k^H, \tag{7}$$

where $\mathbf{d}_k(t,f) = \sum_{\ell=0}^{L_k-1} a_{k,\ell} e^{j2\pi\left(\nu_{k,\ell}^{\mathrm{ut}} t - f\tau_{k,\ell}^{\mathrm{ut}}\right)} \mathbf{d}_{k,\ell} \in \mathbb{C}^{N\times 1}$, $\tau_{k,\ell}^{\mathrm{ut}} = \tau_{k,\ell} - \tau_k^{\min}$. The receiving signal $\mathbf{y}_{k,s,r}$ in (6) can be further expressed as

$$\mathbf{y}_{k,s,r} = \mathbf{H}_{k,s,r}\mathbf{x}_{s,r} + \mathbf{z}_{k,s,r}, \tag{8}$$

where $\mathbf{H}_{k,s,r}$ and $\mathbf{z}_{k,s,r}$ are the channel matrix and additive Gaussian noise of UT k over subcarrier r in OFDM symbol s. In (8), $\mathbf{H}_{k,s,r}$ can be expressed as

$$\mathbf{H}_{k,s,r} = \mathbf{H}_k\left(sT, r\Delta f\right) = \mathbf{d}_{k,s,r}\mathbf{g}_k^H, \tag{9}$$

where $\mathbf{d}_{k,s,r} \triangleq \mathbf{d}_k\left(sT, r\Delta f\right)$. Since the Doppler and delay effects are compensated at each UT, the time and frequency at the satellite and the UTs are assumed to be perfectly synchronized in the following.

D. Satellite Channel's Statistical Properties

For simplicity, we drop the subscripts of OFDM symbol s and subcarrier r in $\mathbf{H}_{k,s,r} = \mathbf{d}_{k,s,r}\mathbf{g}_k^H$. Henceforth, we denote $\mathbf{H}_k = \mathbf{d}_k\mathbf{g}_k^H$ as the DL channel matrix of UT k over a given subcarrier. We assume that the LEO satellite channel $\mathbf{H}_k$ follows Rician distribution as follows

$$\mathbf{H}_k = \mathbf{d}_k\mathbf{g}_k^H = \sqrt{\frac{\kappa_k\beta_k}{\kappa_k+1}}\bar{\mathbf{H}}_k + \sqrt{\frac{\beta_k}{\kappa_k+1}}\tilde{\mathbf{H}}_k, \tag{10}$$

where $\beta_k = \mathbb{E}\left\{\|\mathbf{H}_k\|_{\mathrm{F}}^2\right\} = \mathbb{E}\left\{\|\mathbf{d}_k\|^2\right\}$ is the average channel power, κ_k is the Rician factor. In (10), $\bar{\mathbf{H}}_k = \mathbf{d}_{k,0}\mathbf{g}_k^H$ is the line-of-sight (LoS) part, while $\tilde{\mathbf{H}}_k = \tilde{\mathbf{d}}_k\mathbf{g}_k^H$ is the scattering component. Besides, $\tilde{\mathbf{d}}_k$ is distributed as $\tilde{\mathbf{d}}_k \sim \mathcal{CN}(\mathbf{0}, \mathbf{\Sigma}_k)$ with $\mathrm{tr}(\mathbf{\Sigma}_k) = 1$. These channel parameters $\mathcal{H} \triangleq \{\beta_k, \kappa_k, \mathbf{g}_k, \mathbf{d}_{k,0}, \mathbf{\Sigma}_k\}_{\forall k}$ depend on the operating frequency bands, practical link conditions, etc [20].

III. DL Transmit Design

In this section, building on the signal and channel models in Section II, we investigate the DL transmit strategy by only exploiting slow-varying sCSIT. First, we show that the rank of each UT's transmit covariance matrix is no greater than one for the ergodic sum rate maximization. As a result, the design of transmit covariance matrices can be simplified into that of precoding vectors. Then, by resorting to the minorization-maximization (MM) framework, an algorithm is devised to compute the precoding vectors.

A. Rank-One Property of Transmit Covariance Matrices

For convenience of statement, we drop the subscripts of OFDM symbol s and subcarrier r in $\mathbf{x}_{s,r}$, and denote $\mathbf{x}$ as the $M\times 1$ transmit signal on a given subcarrier. We assume that there are K UTs simultaneously served by the satellite. Let $\mathcal{K} = \{1,\ldots,K\}$ denote the set of UT indices. The transmit signal $\mathbf{x}$ can be written as $\mathbf{x} = \sum_{k=1}^K \mathbf{s}_k$, where $\mathbf{s}_k \in \mathbb{C}^{M\times 1}$ is the transmit signal to UT k. In this paper, $\mathbf{s}_k$ is assumed to be a Gaussian random vector with zero mean and covariance matrix $\mathbf{Q}_k = \mathbb{E}\{\mathbf{s}_k\mathbf{s}_k^H\}$, which is actually the most generally design of transmit signals. We also assume that the transmit signals satisfy the total power constraint, i.e., $\sum_{k=1}^K \mathrm{tr}(\mathbf{Q}_k) \le P$. The DL receiving signal of UT k is given by

$$\mathbf{y}_k = \mathbf{H}_k\sum_{i=1}^K \mathbf{s}_i + \mathbf{z}_k, \tag{11}$$

where $\mathbf{z}_k \in \mathbb{C}^{N\times 1}$ is the additive Gaussian noise at UT k. In addition, $\mathbf{z}_k$ is distributed as $\mathbf{z}_k \sim \mathcal{CN}\left(0, \sigma_k^2\mathbf{I}_N\right)$. The DL ergodic rate of UT k is given by

$$\begin{aligned}\mathcal{I}_k &= \mathbb{E}\left\{\log\det\left(\sigma_k^2\mathbf{I}_N + \mathbf{H}_k\sum_{i=1}^K\mathbf{Q}_i\mathbf{H}_k^H\right)\right\} \\ &\quad - \mathbb{E}\left\{\log\det\left(\sigma_k^2\mathbf{I}_N + \mathbf{H}_k\sum_{i\neq k}\mathbf{Q}_i\mathbf{H}_k^H\right)\right\} \\ &\overset{(a)}{=} \mathbb{E}\left\{\log\left(1 + \frac{\mathbf{g}_k^H\mathbf{Q}_k\mathbf{g}_k\|\mathbf{d}_k\|^2}{\sum_{i\neq k}\mathbf{g}_k^H\mathbf{Q}_i\mathbf{g}_k\|\mathbf{d}_k\|^2 + \sigma_k^2}\right)\right\}, \end{aligned} \tag{12}$$

where (a) follows from $\mathbf{H}_k = \mathbf{d}_k\mathbf{g}_k^H$ and $\det(\mathbf{I}+\mathbf{AB}) = \det(\mathbf{I}+\mathbf{BA})$. The DL sum rate maximization problem can be formulated as

$$\mathcal{P}: \max_{\{\mathbf{Q}_k\}_{k=1}^K} \sum_{k=1}^K \mathcal{I}_k,\ \text{s.t.} \sum_{k=1}^K \mathrm{tr}(\mathbf{Q}_k) \le P,\ \mathbf{Q}_k \succeq \mathbf{0},\ \forall k\in\mathcal{K}. \tag{13}$$

Theorem 1: The optimal $\{\mathbf{Q}_k\}_{k=1}^K$ to problem $\mathcal{P}$ must satisfy $\mathrm{rank}(\mathbf{Q}_k) \le 1$, $\forall k \in \mathcal{K}$.

Theorem 1 reveals that transmitting a single data stream to each UT is optimal for linear transmitters even though each UT is equipped with multiple antennas. Therefore, we can rewrite $\mathbf{Q}_k$ as $\mathbf{Q}_k = \mathbf{w}_k\mathbf{w}_k^H$, where $\mathbf{w}_k \in \mathbb{C}^{M\times 1}$ is the precoding vector of UT k. Then, the transmit signal $\mathbf{s}_k$ is expressed as $\mathbf{s}_k = \mathbf{w}_k s_k$, where s_k is the desired data symbol of UT k with zero mean and unit variance. Consequently, the design of transmit covariance matrices $\{\mathbf{Q}_k\}_{k=1}^K$ is degenerated into that of precoding vectors $\{\mathbf{w}_k\}_{k=1}^K$. By substituting $\mathbf{Q}_k = \mathbf{w}_k\mathbf{w}_k^H$ into (12), we have

$$\mathcal{I}_k = \mathbb{E}\left\{\log\left(1 + \frac{\left|\mathbf{w}_k^H\mathbf{g}_k\right|^2\|\mathbf{d}_k\|^2}{\sum_{i\neq k}\left|\mathbf{w}_i^H\mathbf{g}_k\right|^2\|\mathbf{d}_k\|^2 + \sigma_k^2}\right)\right\} \triangleq \mathcal{R}_k. \tag{14}$$

We use $\mathcal{R}_k$ to represent the DL ergodic rate of UT k, since $\mathcal{R}_k$ has become a function of the precoding vectors $\{\mathbf{w}_k\}_{k=1}^K$. Then, the transmit covariance matrix optimization problem $\mathcal{P}$ in (13) can be simplified into the precoding vector optimization problem as follows

$$\mathcal{S}:\ \max_{\mathbf{W}} \sum_{k=1}^K \mathcal{R}_k,\ \text{s.t.}\ \sum_{k=1}^K \|\mathbf{w}_k\|^2 \le P, \tag{15}$$

where $\mathbf{W} = [\mathbf{w}_1\ \cdots\ \mathbf{w}_K] \in \mathbb{C}^{M\times K}$. Note that the power constraint in (15) must be met with equality at the optimum of $\mathcal{S}$, i.e., $\sum_{k=1}^K \|\mathbf{w}_k\|^2 = P$. Otherwise, we can always scale up $\{\mathbf{w}_k\}_{k=1}^K$, thus improving the DL ergodic sum rate and contradicting the optimality.

B. Precoding Vector Design

In this subsection, we compute the precoding vectors that can maximize the ergodic sum rate under the total power constraint. Due to the non-convexity of the precoding vector optimization problem $\mathcal{S}$ in (15), it is generally challenging to derive the precoding vectors analytically.

In the following, we devise an algorithm based on the MM framework in [21] to obtain a locally optimal solution of $\mathcal{S}$. In each iteration, we replace the DL ergodic rate $\mathcal{R}_k$ with one of its concave minorizing functions. Then, a locally optimal solution to $\mathcal{S}$ is guaranteed to be achieved by iteratively solving a sequence of convex problems.

Let $\mathbf{c}_k \in \mathbb{C}^{N\times 1}$ be the linear receiver of UT k. Then, the recovered data symbol at UT k is given by $\hat{s}_k = \mathbf{c}_k^H \mathbf{y}_k = \mathbf{c}_k^H \mathbf{d}_k \mathbf{g}_k^H \mathbf{w}_k s_k + \sum_{i\neq k}^K \mathbf{c}_k^H \mathbf{d}_k \mathbf{g}_k^H \mathbf{w}_i s_i + \mathbf{c}_k^H \mathbf{z}_k$. Define the mean-square error (MSE) of UT k as $\mathrm{MSE}_k \triangleq \mathbb{E}\{|\hat{s}_k - s_k|^2\} = \sum_{i=1}^K |\mathbf{w}_i^H \mathbf{g}_k|^2 |\mathbf{c}_k^H \mathbf{d}_k|^2 + \sigma_k^2 \|\mathbf{c}_k\|^2 - 2\Re\{\mathbf{g}_k^H \mathbf{w}_k \cdot \mathbf{c}_k^H \mathbf{d}_k\} + 1$. The optimal $\mathbf{c}_k$ is given by '

$$\mathbf{c}_{\mathrm{mmse},k} = \arg\min_{\mathbf{c}_k} \mathrm{MSE}_k = \frac{\mathbf{g}_k^H \mathbf{w}_k}{\sigma_k^2 + \sum_{i=1}^K \left|\mathbf{w}_i^H \mathbf{g}_k\right|^2 \|\mathbf{d}_k\|^2} \cdot \mathbf{d}_k. \tag{16}$$

The minimum MSE (MMSE) of UT k achieved by $\mathbf{c}_{\mathrm{mmse},k}$ is given by

$$\mathrm{MMSE}_k = 1 - \frac{\left|\mathbf{w}_k^H \mathbf{g}_k\right|^2 \|\mathbf{d}_k\|^2}{\sigma_k^2 + \sum_{i=1}^K \left|\mathbf{w}_i^H \mathbf{g}_k\right|^2 \|\mathbf{d}_k\|^2}. \tag{17}$$

Then, $\mathcal{R}_k$ can be expressed as $\mathcal{R}_k = -\mathbb{E}\{\log \mathrm{MMSE}_k\}$. Hereafter, we use $(\cdot)^{(n)}$ to denote the argument in the nth iteration. Due to the concavity of logarithm functions, a minoring function of $\mathcal{R}_k$ is given by

$$\begin{aligned} \mathcal{R}_k &\geq \mathcal{R}_k^{(n)} - \mathbb{E}\left\{\frac{\mathrm{MMSE}_k - \mathrm{MMSE}_k^{(n)}}{\mathrm{MMSE}_k^{(n)}}\right\} \\ &\overset{\text{(a)}}{\geq} \mathcal{R}_k^{(n)} + 1 - \mathbb{E}\left\{\frac{\mathrm{MSE}_k}{\mathrm{MMSE}_k^{(n)}}\right\} \triangleq g_k^{(n)}, \end{aligned} \tag{18}$$

where (a) follows from $\mathrm{MMSE}_k \leq \mathrm{MSE}_k$ for all $\mathbf{c}_k$. To make the inequality in (18) hold with equality at $\mathbf{W}^{(n)}$, we choose the receiver $\mathbf{c}_k$ in MSE_k as $\mathbf{c}_{\mathrm{mmse},k}^{(n)}$. By substituting $\mathbf{c}_{\mathrm{mmse},k}^{(n)}$ into MSE_k, we have

$$\mathbb{E}\left\{\frac{\mathrm{MSE}_k}{\mathrm{MMSE}_k^{(n)}}\right\} = a_k^{(n)} \sum_{i=1}^K |\mathbf{w}_i^H \mathbf{g}_k|^2 - 2\Re\{\mathbf{w}_k^H \mathbf{g}_k \cdot b_k^{(n)}\} + c_k^{(n)}, \tag{19}$$

where $a_k^{(n)} = \mathbb{E}\left\{\frac{|\mathbf{d}_k^H \mathbf{c}_{\mathrm{mmse},k}^{(n)}|^2}{\mathrm{MMSE}_k^{(n)}}\right\}$, $b_k^{(n)} = \mathbb{E}\left\{\frac{\mathbf{d}_k^H \mathbf{c}_{\mathrm{mmse},k}^{(n)}}{\mathrm{MMSE}_k^{(n)}}\right\}$ and $c_k^{(n)} = \mathbb{E}\left\{\frac{\sigma_k^2 \|\mathbf{c}_{\mathrm{mmse},k}^{(n)}\|^2 + 1}{\mathrm{MMSE}_k^{(n)}}\right\}$.

By making use of the minorizing function $g_k^{(n)}$ in (18), the precoding vectors $\{\mathbf{w}_k^{(n+1)}\}_{k=1}^K$ can be obtained by solving the following convex quadratic program

$$\min_{\mathbf{W}} \sum_{k=1}^K \left(\sum_{i=1}^K a_i^{(n)} |\mathbf{w}_k^H \mathbf{g}_i|^2 - 2\Re\{\mathbf{w}_k^H \mathbf{g}_k \cdot b_k^{(n)}\} \right) \tag{20a}$$

Algorithm 1 Precoder design algorithm for solving $\mathcal{S}$.

Input: Initialize precoding vector $\mathbf{w}_k^{(0)} = \mathbf{w}_k^{\mathrm{init}}$, $k \in \mathcal{K}$, iteration index $n = 0$.
Output: Precoding vectors $\{\mathbf{w}_k\}_{k=1}^K$.

```
while 1 do
    Calculate a_k^(n) and b_k^(n) for all k ∈ K.
    Update {w_k^(n+1)}_{k=1}^K with (21).
    if n ≥ N_iter − 1 or |Σ_{k=1}^K R_k^(n+1) − Σ_{k=1}^K R_k^(n)| < ε then
        Set w_k := w_k^(n+1), ∀k ∈ K, break.
    else
        Set n := n + 1.
    end if
end while
```

$$\text{s.t.} \sum_{k=1}^K \|\mathbf{w}_k\|^2 \leq P. \tag{20b}$$

The optimal solution to (20) can be obtained as

$$\mathbf{w}_k^{(n+1)} = \left(\sum_{i=1}^K a_i^{(n)} \mathbf{g}_i \mathbf{g}_i^H + \mu^{(n)} \mathbf{I}_M \right)^{-1} \mathbf{g}_k \cdot b_k^{(n)}, \ \forall k, \tag{21}$$

where $\mu^{(n)} \geq 0$ is chosen such that $\sum_{k=1}^K \|\mathbf{w}_k^{(n+1)}\|^2 = P$. The precoding vector optimization algorithm for solving $\mathcal{S}$ is presented in Algorithm 1. With the help of the LEO satellite channel characteristics, only the scalar parameters $\{a_k^{(n)}, b_k^{(n)}\}_{k=1}^K$ are required for computation in each iteration.

IV. Simulation Results

In this section, we show the simulation results to demonstrate the proposed DL transmit designs in a massive MIMO LEO SATCOM system. The simulation parameters are listed in TABLE I. The paired space angles $\{\tilde{\boldsymbol{\theta}}_k\}_{k=1}^K$ are generated by following the uniform distribution in the circle region $\{(x, y) : x^2 + y^2 \leq \sin^2 \vartheta_{\max}\}$. The elevation angle seen at UT k is given by $\alpha_k = \cos^{-1}\left(\frac{R_s}{R_e} \sin \vartheta_k\right)$ [20], where R_e is the earth radius, $R_s = R_e + H$ is the orbit radius. The distance between the satellite and UT k is given by $D_k = \sqrt{R_e^2 \sin^2 \alpha_k + H^2 + 2HR_e} - R_e \sin \alpha_k$ [1]. Define the per-antenna gains of the UPAs at the satellite and each UT as G_{sat} and G_{ut}, respectively. The random vector $\mathbf{d}_k$ in (10) is generated on the basis of $\mathbf{d}_k(t, f)$ in (7), where the first path is for the LoS part $\mathbf{d}_{k,0} = \mathbf{d}(\boldsymbol{\varphi}_{k,0})$ and the remaining $L_k - 1$ paths are for the scattering part $\tilde{\mathbf{d}}_k$. Each UT's UPA is assumed to be placed horizontally, and thus $\boldsymbol{\varphi}_{k,0}$ satisfies $\sin \varphi_{k,0}^{\mathrm{y}'} \sin \varphi_{k,0}^{\mathrm{x}'} = \sin \alpha_k$, e.g., $\varphi_{k,0}^{\mathrm{x}'} = 90°$ and $\varphi_{k,0}^{\mathrm{y}'} = \alpha_k$. In $\tilde{\mathbf{d}}_k$, the path gains $\{a_{k,\ell}\}_{\ell=1}^{L_k-1}$ are generated by using the exponential power delay profile, and the paired AoAs $\{\boldsymbol{\varphi}_{k,\ell}\}_{\ell=1}^{L_k-1}$ are generated by using the wrapped Gaussian power angle spectrum [1, Section 6]. In addition, the pathloss, shadow fading and Rician factors are also generated based on the channel models in [1, Section 6]. The noise variance is given by $\sigma_k^2 = k_{\mathrm{B}} T_{\mathrm{n}} B$ where $k_{\mathrm{B}} = 1.38 \times 10^{-23}$ $\mathrm{J \cdot K^{-1}}$ is the Boltzmann constant, T_{n} is the noise temperature and B is the system bandwidth.

In Fig. 1, the convergence performance of Algorithm 1 is shown. It is observed that Algorithm 1 will converge to a locally

TABLE I: Simulation Parameters

Parameters	Values
Earth radius R_e	6378 km
Orbit altitude H	1000 km
Central frequency f_c	4 GHz
Bandwidth B	50 MHz
Noise temperature T_{n}	290 K
Number of antennas $M_{\mathrm{x}} \times M_{\mathrm{y}}$, $N_{\mathrm{x}'} \times N_{\mathrm{y}'}$	12×12, 6×6
Antenna spacing d_{x}, d_{y}, $d_{\mathrm{x}'}$, $d_{\mathrm{y}'}$	λ, λ, $\frac{\lambda}{2}$, $\frac{\lambda}{2}$
Per-Antenna gain G_{sat}, G_{ut}	3 dB, 0 dB
Maximum nadir angle $\vartheta_{\max}$	30°
Number of UTs K	100
Transmit power P	10 dBW – 30 dBW

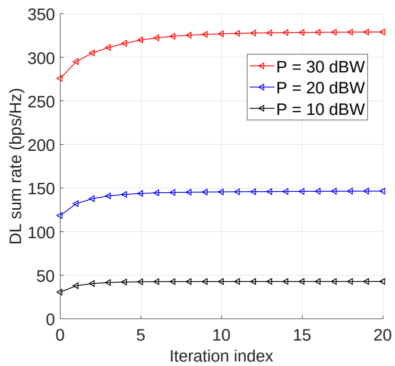

Fig. 1: Convergence of Algorithm 1 for different P.

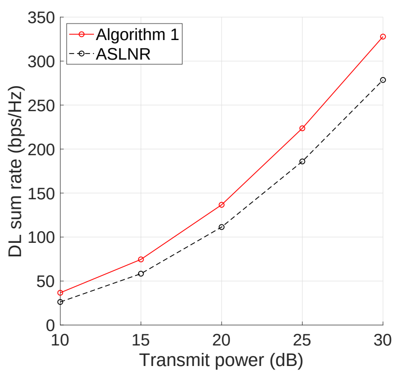

Fig. 2: DL sum rate performance of Algorithm 1.

optimum within a small number of iterations. In Fig. 2, the sum rate performance of Algorithm 1 and ASLNR precoding vectors $\{\mathbf{w}_k^{\mathrm{aslnr}}\}_{k=1}^K$ [16] is shown. The ASLNR precoding vectors $\mathbf{w}_k^{\mathrm{aslnr}}$'s can be written as $\mathbf{w}_k^{\mathrm{aslnr}} = \sqrt{p_k} \cdot \frac{\mathbf{T}_k^{-1}\mathbf{g}_k}{\|\mathbf{T}_k^{-1}\mathbf{g}_k\|}$, where $\mathbf{T}_k = \sum_{i=1}^K \beta_i \mathbf{g}_i \mathbf{g}_i^H + \frac{\sigma_k^2}{p_k}\mathbf{I}_M$, and p_k is set as $p_k = \frac{P}{K}$ for simplicity. It can be observed that Algorithm 1 has a performance gain of about 2 dB at $P = 30$ dBW compared with the conventional ASLNR precoding vectors.

V. Conclusion

In this paper, we studied the DL transmit strategy with sCSIT in massive MIMO LEO SATCOM systems. First, we established the massive MIMO LEO satellite channel model, where the satellite and the UTs are both equipped with UPAs. Then, we showed that it is sufficient to transmit a single data stream to each UT for ergodic sum rate maximization. Hence, the design of transmit covariance matrices is simplified into that of precoding vectors without loss of optimality. Afterwards, we devised an algorithm to compute the precoding vectors. Finally, we demonstrated the performance gains of the proposed DL transmit design with the simulation results.

References

[1] 3GPP TR 38.811, “Study on new radio (NR) to support non-terrestrial networks (Release 15),” Sophia Antipolis Valbonne, France, V15.3.0, Jul. 2020.

[2] B. Di, L. Song, Y. Li, and H. V. Poor, “Ultra-dense LEO: Integration of satellite access networks into 5G and beyond,” *IEEE Wireless Commun.*, vol. 26, no. 2, pp. 62–69, Apr. 2019.

[3] Y. Su, Y. Liu, Y. Zhou, J. Yuan, H. Cao, and J. Shi, “Broadband LEO satellite communications: Architectures and key technologies,” *IEEE Wireless Commun.*, vol. 26, no. 2, pp. 55–61, Apr. 2019.

[4] G. Maral and M. Bousquet, *Satellite Communications Systems: Systems, Techniques and Technology*, 5th ed. Chichester, UK: Wiley, 2009.

[5] A. I. Pérez-Neira, M. A. Vázquez, M. R. B. Shankar, S. Maleki, and S. Chatzinotas, “Signal processing for high-throughput satellites: Challenges in new interference-limited scenarios,” *IEEE Signal Process. Mag.*, vol. 36, no. 4, pp. 112–131, Jul. 2019.

[6] G. Zheng, S. Chatzinotas, and B. Ottersten, “Generic optimization of linear precoding in multibeam satellite systems,” *IEEE Trans. Wireless Commun.*, vol. 11, no. 6, pp. 2308–2320, Jun. 2012.

[7] D. Christopoulos, S. Chatzinotas, and B. Ottersten, “Multicast multigroup precoding and user scheduling for frame-based satellite communications,” *IEEE Trans. Wireless Commun.*, vol. 14, no. 9, pp. 4695–4707, Sep. 2015.

[8] V. Joroughi, M. A. Vázquez, and A. I. Pérez-Neira, “Precoding in multigateway multibeam satellite systems,” *IEEE Trans. Wireless Commun.*, vol. 15, no. 7, pp. 4944–4956, Jul. 2016.

[9] T. L. Marzetta, “Noncooperative cellular wireless with unlimited numbers of base station antennas,” *IEEE Trans. Wireless Commun.*, vol. 9, no. 11, pp. 3590–3600, Nov. 2010.

[10] W. Hong, Z. H. Jiang, C. Yu, J. Zhou, P. Chen, Z. Yu, H. Zhang, B. Yang, X. Pang, M. Jiang, Y. Cheng, M. K. T. Al-Nuaimi, Y. Zhang, J. Chen, and S. He, “Multibeam antenna technologies for 5G wireless communications,” *IEEE Trans. Antennas Propag.*, vol. 65, no. 12, pp. 6231–6249, Dec. 2017.

[11] P. Angeletti and R. De Gaudenzi, “A pragmatic approach to massive MIMO for broadband communication satellites,” *IEEE Access*, vol. 8, pp. 132 212–132 236, 2020.

[12] X. Q. Gao, B. Jiang, X. Li, A. B. Gershman, and M. R. McKay, “Statistical eigenmode transmission over jointly correlated MIMO channels,” *IEEE Trans. Inf. Theory*, vol. 55, no. 8, pp. 3735–3750, Aug. 2009.

[13] A. Adhikary, J. Nam, J. Ahn, and G. Caire, “Joint spatial division and multiplexing – The large-scale array regime,” *IEEE Trans. Inf. Theory*, vol. 59, no. 10, pp. 6441–6463, Oct. 2013.

[14] C. Sun, X. Q. Gao, S. Jin, M. Matthaiou, Z. Ding, and C. Xiao, “Beam division multiple access transmission for massive MIMO communications,” *IEEE Trans. Commun.*, vol. 63, no. 6, pp. 2170–2184, Jun. 2015.

[15] A.-A. Lu, X. Q. Gao, W. Zhong, C. Xiao, and X. Meng, “Robust transmission for massive MIMO downlink with imperfect CSI,” *IEEE Trans. Commun.*, vol. 67, no. 8, pp. 5362–5376, Aug. 2019.

[16] L. You, K.-X. Li, J. Wang, X. Q. Gao, X.-G. Xia, and B. Ottersten, “Massive MIMO transmission for LEO satellite communications,” *IEEE J. Sel. Areas Commun.*, vol. 38, no. 8, pp. 1851–1865, Aug. 2020.

[17] I. Ali, N. Al-Dhahir, and J. E. Hershey, “Doppler characterization for LEO satellites,” *IEEE Trans. Commun.*, vol. 46, no. 3, pp. 309–313, Mar. 1998.

[18] A. Papathanassiou, A. K. Salkintzis, and P. T. Mathiopoulos, “A comparison study of the uplink performance of W-CDMA and OFDM for mobile multimedia communications via LEO satellites,” *IEEE Personal Communications*, vol. 8, no. 3, pp. 35–43, Jun. 2001.

[19] A. Guidotti, A. Vanelli-Coralli, T. Foggi, G. Colavolpe, M. Caus, J. Bas, S. Cioni, and A. Modenini, “LTE-based satellite communications in LEO mega-constellations,” *Int. J. Satell. Commun. Netw.*, vol. 37, no. 4, pp. 316–330, Jun. 2019.

[20] E. Lutz, M. Werner, and A. Jahn, *Satellite Systems for Personal and Broadband Communications*. Berlin, Heidelberg: Springer, 2000.

[21] D. R. Hunter and K. Lange, “A tutorial on MM algorithms,” *The American Statistician*, vol. 58, no. 1, pp. 30–37, 2004.